Journal of Magnetic Resonance **140,** 9–16 (1999)
Article ID jmre.1999.1826, available online at http://www.idealibrary.com on IDEAL®

Spectroscopy from Proton Spin Magnetization Evolution in Their Rotating Frame: A Study of Small Tunneling Splitting

A. Damyanovich,* J. Peternelj,† and M. M. Pintar‡

*Department of Medical Imaging, University of Toronto, Toronto, Ontario M5S 1A1, Canada; †Faculty of Civil and Geodetic Engineering, University of Ljubljana and Institute J. Stefan, Ljubljana, Slovenia; and ‡Department of Physics, University of Waterloo, Waterloo, Ontario N2L 3G1, Canada

Received November 18, 1998; revised May 17, 1999

The time evolution of proton Zeeman magnetization in the rotating frame at exact resonance, $\omega = \omega_0$, is evaluated for an isolated tunneling methyl group CH_3. The Fourier transform of this evolution in time is calculated and both its real and imaginary components are presented. It is shown that the real component does not depend significantly on the strength of the preparation pulse when the tunneling splitting of the methyl rotator ground state is less than 100 kHz. It is also found that the imaginary component of the transform is inversely proportional to the strength of the preparation RF pulse. This is a consequence of the partial dephasing of proton spins during the preparation pulse. The results of the calculation compare well with the experimental spectra of CH_3CD_2I. © 1999 Academic Press

INTRODUCTION

At low temperatures symmetric atomic groups, e.g., CH_3 and NH_4, embedded in a solid lattice are often in a state of tunneling between equivalent neighboring potential minima. As a consequence, the degeneracy of their ground state is, in general, removed; it is said that the ground state is split by tunneling. The magnitude of this splitting is of interest because it relates to the strength and symmetry of the crystal potential and is also influenced by the interaction between different atomic groups (*1*). This splitting, which is written in terms of the tunneling frequency ω_T as $\hbar\omega_T$, can be detected, in the energy range 10^{-10} to 10^{-9} eV, accurately by NMR.

Initially, the information on ω_T was derived from NMR lineshape. This approach, which is experimentally the easiest, unfortunately requires a different lineshape analysis for each value of ω_T (*2*).

Another method is the level-crossing spectroscopy in the rotating frame (*3*). Its main advantage is good signal-to-noise ratio (S/N) and has, when level-crossing occurs in the magic angle tilted rotating frame, also an excellent resolution (*4*). Unfortunately, the search for level-crossing resonances in magic frame requires a different off-resonance field for each different RF amplitude along the magic direction (*5*). This is very time consuming. An extension of the level-crossing in the rotating frame to much larger values of tunneling splitting has been realized by the so-called dipolar-driven NMR (*6*). This method, which has an excellent S/N, is experimentally demanding because it first establishes Zeeman polarization in a high magnetic field and then requires the sample to be dropped into a different magnetic field of low intensity. This is not unlike the spin-locking in the rotating frame. However, the rotating frame RF field is limited to $\leq 10^{-2}$ T, while there is no restriction for the low magnetic field of the dipolar-driven method.

The last method, which is also the subject of this paper, is the magnetization evolution following establishing a nonequilibrium in the rotating frame by spin-locking the spins and monitoring their evolution toward semiequilibrium (*7*). The Fourier transform of this evolution in time gives the spectrum. This technique, while similar to both level-crossing methods, is experimentally much easier. It offers also an excellent resolution when the evolution is monitored in a magic angle tilted rotating frame, but it has a lower S/N in comparison with both level-crossing methods. A recent extension of this method to two time domains, one in the rotating frame and the other in the high field following the end of the RF pulse, allows also for a nonmagnetic ($\Delta M = 0$) detection of the tunneling frequency (*8*).

We propose to investigate the time evolution of the proton magnetization, of an ensemble of isolated methyl groups embedded in a crystal lattice in an external dc magnetic field $\vec{H}_0$, and exposed to RF pulses which are short in comparison with the spin–lattice relaxation time. The pulse sequence for the measurement of $M_x(t)$, the Zeeman magnetization in the rotating frame at exact resonance, is as follows. The first pulse is the so-called 90° pulse. Its phase defines the orientation of the transverse axes in the frame of reference which is rotating about the direction of $\vec{H}_0$, which itself is pointing along the z-axis of the laboratory coordinate frame. By convention the RF field, which causes the 90° rotation, is directed along the y-axis. The RF spin-locking pulse which follows immediately after is shifted in phase by 90° with respect to the 90° pulse and is thus along the x-axis of the rotating frame.

Once the spin-locking pulse is switched off, the free induction decay (FID) in the high field begins. Because of the

1090-7807/99 $30.00

instrumental dead time, a 10-μs delay is usually chosen before the FID amplitudes are recorded.

The density matrix for spins in the 90° tilted rotating frame follows from

$$i\hbar \frac{\partial \sigma}{\partial t} = [H, \sigma], \qquad [1]$$

where H is the Hamiltonian of the system. Equation [1] must be supplemented by the initial condition $\sigma(t = 0) \equiv \sigma(0)$, imposed on the density matrix; the time $t = 0$ refers to the instant when the RF field pulse is switched on. It is a common practice to assume that a good approximation for $\sigma(0)$ is

$$\sigma(0) \propto e^{-\beta_z H_z - \beta_L (H_R + H_D^{00})}, \qquad [2]$$

where $\beta = 1/kT$, and the Zeeman temperature T_Z in the rotating frame equals the lattice temperature T_L times H_1/H_0. The term H_D^{00} is the secular part of the dipolar interaction in the rotating frame (see below). Time evolution of $M_x(t)$ in the rotating frame at exact resonance and based on the above initial condition has been studied previously (*7*). The purpose of the present investigation is to examine whether the use of the initial condition [2] entails any loss of spectroscopic information that would be otherwise available from the calculated $M_x(t)$. To this end we assume only, instead of employing [2], that prior to the application of the 90° pulse, the Zeeman-rotational system is in thermal equilibrium with the lattice. Following this, the time evolution of the spin system during the 90° pulse will be taken into account, resulting in a modified initial condition compared to [2]. This is mandatory whenever the magnitude of the 90° pulse is comparable to the strength of the spin-locking field pulse.

The calculated expressions for $M_x(t)$ will always refer to the end of the field pulse. In actual experiments, however, the recorded time "point" on the FID is delayed by for a time τ after the end of the field pulse. Thus, to compare the experimental results consistently with the calculated ones, the evolution of the Zeeman-rotational system during this time interval τ (when spins evolve in the laboratory frame) should be considered as well. A significant consequence of this delay was reported recently (*8*).

The experimental data on CH_3CD_2I corroborate the theoretical results conclusively.

THE HAMILTONIAN OF THE SYSTEM AND THE EQUATION OF MOTION FOR THE DENSITY MATRIX IN THE ROTATING FRAME

The Hamiltonian describing the dynamics of an isolated methyl group in the laboratory frame, and on a timescale short compared to the spin–lattice relaxation time, is

$$H = H_Z + H_R + H_D + H_{RF}(t). \qquad [3]$$

The Zeeman Hamiltonian reads

$$H_Z = -\hbar \omega_0 I_z, \qquad [4]$$

where $I_z = I_{1z} + I_{2z} + I_{3z}$ is the z-component of the total spin of the methyl group protons, while $\omega_0 = \gamma_p H_0$ is the proton Zeeman frequency. The rotational Hamiltonian H_R does not have to be given explicitly; it is sufficient to recall its threefold symmetry and that the hindering potential V_3 is large enough to limit the tunneling frequency of the methyl group to be comparable to the dipolar frequency $\omega_D = \gamma_p^2 \hbar / R_0^3$. Taking the value of the proton–proton distance $R_0 \cong 1.78$ A, we obtain $\omega_D = 134$ kHz or $\omega_D/\gamma_p \cong 5$ G.

The dipole–dipole interaction written, with a minor change, in the form as given in Ref. (*9*), is

$$H_D = \hbar \omega_D \sum_{k=-2}^{2} (-1)^k \sum_{i<j} U_{ij}^{-k} V_{ij}^{k}. \qquad [5]$$

The operators U_{ij}^{-k} and V_{ij}^{k} are

$$U_{ij}^{-k} = (6\pi/5)^{1/2} Y_2^{-k}(\theta_{ij}, \varphi_{ij}), \qquad [6]$$

with the spherical harmonics defined in (*9*), and the polar angles $(\theta_{ij}, \varphi_{ij})$ determining the orientation of the proton–proton vector $\vec{R}_{ij}$. The spin operators are (*9*)

$$V_{ij}^{0} = -(8/3)^{1/2}[I_i^0 I_j^0 - \tfrac{1}{4}(I_i^{+1} I_j^{-1} + I_i^{-1} I_j^{+1})], \qquad [7a]$$

$$V_{ij}^{\pm 1} = \pm (I_i^0 I_j^{\pm 1} + I_i^{\pm 1} I_j^0), \qquad [7b]$$

$$V_{ij}^{\pm 2} = -I_i^{\pm 1} I_j^{\pm 1}, \qquad [7c]$$

where $I_i^0 \equiv I_{iz}$ and $I_i^{\pm 1} = I_{ix} \pm i I_{iy}$.

The radiofrequency field applied to the sample is a rotating transverse magnetic field. The corresponding interaction Hamiltonian is

$$H_{RF}(t) = -\hbar \omega_1 (I_x \cos \omega_0 t - I_y \sin \omega_0 t), \qquad [8]$$

$\omega_1 = \gamma_p H_1$, $I_x = I_{1x} + I_{2x} + I_{3x}$ and similarly for I_y.

The equation of motion for the density matrix ρ_r in the rotating frame is approximated by

$$i\hbar \frac{\partial \rho_r}{\partial t} = [-\hbar \omega_1 I_x + H_R + \hbar \omega_D \sum_{i<j} U_{ij}^0 V_{ij}^0, \rho_r]. \qquad [9]$$

It is related to the density matrix ρ in the laboratory frame by the unitary transformation

$$\rho = e^{i\omega_0 t I_z}\rho_r e^{-i\omega_0 t I_z}. \quad [10]$$

Next, the 90° tilted rotating frame, also called on-resonance rotating frame, is introduced by making the transformation

$$\sigma = e^{i(\pi/2)I_y}\rho_r e^{-i(\pi/2)I_y}, \quad [11]$$

with the resulting equation of motion for σ

$$i\hbar\frac{\partial\sigma}{\partial t} = [H_0 + V, \sigma], \quad [12]$$

where

$$H_0 = -\hbar\omega_1 I_z + H_R + H_D^{00}, \quad [13]$$

$$H_D^{00} = d_{00}\hbar\omega_D \sum_{i<j} U_{ij}^0 V_{ij}^0, \quad [14]$$

and

$$V = \sum_{k\neq 0} d_{0k}(\hbar\omega_D \sum_{i<j} U_{ij}^0 V_{ij}^k) \equiv \sum_{k\neq 0} d_{0k}V^k. \quad [15]$$

The coefficients d_{0k}, for $-2 \le k \le 2$, are the $\theta = \pi/2$ values of the expressions (*9*)

$$d_{00}(\theta) = (3\cos^2\theta - 1)/2, \quad [16a]$$

$$d_{0\pm1}(\theta) = \pm(3/2)^{1/2}\sin\theta\cos\theta, \quad [16b]$$

$$d_{0\pm2}(\theta) = (3/8)^{1/2}\sin^2\theta. \quad [16c]$$

DIAGONALIZATION OF H_0

We shall diagonalize H_0 in the basis of the eigenstates of $-\hbar\omega_1 I_z + H_R$, which we write as

$$\psi_{\nu,M}(\gamma) = \phi_\nu(\gamma)\chi_{\tilde{\nu}}(I, M) \equiv |\nu M\rangle. \quad [17]$$

The rotational components $\phi_\nu(\gamma)$, where γ is the angle describing the rotation of the methyl group around its symmetry axis, are

$$\phi_\nu(\gamma) = \frac{1}{\sqrt{3}}\left[\phi_0(\gamma) + e^{-i(2\pi/3)s}\phi_0\left(\gamma + \frac{2\pi}{3}\right) + e^{i(2\pi/3)s}\phi_0\left(\gamma - \frac{2\pi}{3}\right)\right]. \quad [18]$$

$\phi_0(\gamma)$ are the so-called pocket states and $s = 0$, 1, and -1 correspond to $\nu = A$, E_a, and E_b, respectively, which, in turn, label the irreducible representations of the point group C_3 (*1*). As usual, we will restrict ourselves to low temperatures, such that only the lowest three rotational levels are appreciably populated. The symmetry adapted spin states are (*1*)

$$\chi_A\left(\frac{3}{2}, \frac{3}{2}\right) = |\alpha\alpha\alpha\rangle,$$

$$\chi_A\left(\frac{3}{2}, \frac{1}{2}\right) = \frac{1}{\sqrt{3}}[|\alpha\alpha\beta\rangle + |\alpha\beta\alpha\rangle + |\beta\alpha\alpha\rangle],$$

$$\chi_{E_a}\left(\frac{1}{2}, \frac{1}{2}\right) = \frac{1}{\sqrt{3}}[|\alpha\alpha\beta\rangle + \epsilon|\alpha\beta\alpha\rangle + \epsilon^*|\beta\alpha\alpha\rangle], \quad [19]$$

where $\epsilon = e^{i2\pi/3}$ and the asterisk denotes complex conjugate value. It holds that $\chi_{Eb}(1/2, M) = \chi^*_{Ea}(1/2, M)$. In addition α and β represent the z-components $\frac{1}{2}$ and $-\frac{1}{2}$, respectively, of the proton spin, and the spin states with negative values of M are obtained from [19] by interchanging α and β. The Pauli principle imposed on the protons demands that only combinations $(\nu, \tilde{\nu}) \in (AA, E_aE_b, E_bE_a)$ occur in [17].

The Hamiltonian identical to H_0, apart from the factor d_{00} in [14], has been discussed previously by Andrew and Bersohn (without the H_R term) (*10*) and Apaydin and Clough (*11*). Consequently, repeating and extending their calculation, we obtain

$$H_0|A, \pm3/2\rangle = \left[\mp\frac{3}{2}\hbar\omega_1 - 2\hbar a\right]|A, \pm3/2\rangle, \quad [20a]$$

$$H_0|E, \pm1/2\rangle = \left[\mp\frac{1}{2}\hbar\omega_1 + \hbar\Delta\right]|E, \pm1/2\rangle, \quad [20b]$$

$$H_0|(AE)_\pm, M\rangle = \left[-M\hbar\omega_1 + \hbar\Delta + \left(\hbar a - \frac{1}{2}\hbar\Delta\right) \pm b^{1/2}\right]|(AE)_\pm, M\rangle. \quad [20c]$$

The eigenstate $|A, \pm3/2\rangle$ is defined by [17] and [19], while

$$|E, \pm1/2\rangle = \frac{1}{\sqrt{2}}[\epsilon^*|E_a, \pm1/2\rangle - \epsilon|E_b, \pm1/2\rangle], \quad [20d]$$

and

$$|(AE)_\pm, M\rangle = C_\pm[\alpha_\pm|A, M\rangle - \epsilon^*|E_a, M\rangle - \epsilon|E_b, M\rangle], \text{ for } M = \pm1/2. \quad [20e]$$

The zero of energy was chosen such that $\langle A, M|H_R|A, M\rangle = 0$, and $\langle E_{a,b}, M|H_R|E_{a,b}, M\rangle = \hbar\Delta$. The quantities introduced above are

$$a = \tfrac{3}{16} d_{00}\omega_D(1 - 3\cos^2\beta), \quad [21a]$$

$$b = \left(a - \frac{1}{2}\Delta\right)^2 + 2\left(a + \frac{3}{8}d_{00}\omega_D\right)^2, \quad [21b]$$

$$c_\pm = \frac{-2\left(a + \frac{3}{8}d_{00}\omega_D\right)}{\left\{8b^{1/2}\left[b^{1/2} \pm \left(a - \frac{1}{2}\Delta\right)\right]\right\}^{1/2}}, \quad [21c]$$

$$\alpha_\pm = \frac{\left(a - \frac{1}{2}\Delta\right) \pm b^{1/2}}{a + \frac{3}{8}d_{00}\omega_D}, \quad [21d]$$

where β denotes the angle between the external magnetic field $\vec{H}_0$ and the symmetry axis of the methyl group. Inspection of the results reveals that the eigenvalues given in [20] agree, except for the multiplying factor d_{00} and the uniform shift of all the levels, with the corresponding values obtained by Clough and Apaydin (*11*, see p. 934).

TIME EVOLUTION OF THE ZEEMAN POLARIZATION IN THE ROTATING FRAME

The equation of motion [12] for σ is solved by using the interaction representation defined by

$$\sigma_I(t) = e^{(i/\hbar)H_0 t}\sigma(t)e^{-(i/\hbar)H_0 t}. \quad [22]$$

In the interaction picture the density matrix, $\sigma_I(t)$, is given, to the second order in the dipolar interaction V, as

$$\sigma_I(t) = \sigma_I(0) + \left(-\frac{i}{\hbar}\right)\int_0^t dt_1[V(t_1), \sigma_I(0)] + \left(-\frac{i}{\hbar}\right)^2\int_0^t dt_1\int_0^{t_1} \times dt_2[V(t_1), [V(t_2), \sigma_I(0)]] + \cdots, \quad [23]$$

where

$$V(t) = e^{(i/\hbar)H_0 t}Ve^{-(i/\hbar)H_0 t}, \quad [24]$$

and, of course, $\sigma_I(0) \equiv \sigma(0)$.

The initial density matrix $\sigma(0)$ describes the state of the system in the 90° tilted rotating frame immediately after the 90° pulse was switched off. Prior to the application of the 90° pulse the spin-rotational system is assumed to be in thermal equilibrium with the lattice at temperature T_L. It is also well known that, when the strength of the 90° pulse H_1' is large compared to the strength of the rotating transverse magnetic field H_1 which, in turn, is assumed large compared to ω_D/γ_p, it is permissible to consider the 90° pulse as a rotation operator. Its effect is to rotate all the spins around the y-axis. On the other hand, if H_1' is comparable to H_1, spin dephasing during the 90° pulse due to dipole–dipole interaction should be taken into account in order to analyze the experimental data consistently.

Assuming that the RF field corresponding to the 90° pulse is along the negative y-axis we obtain, by employing the high temperature approximation and keeping only terms up to first order in dipolar interaction, the following form

$$\sigma(0) = \sigma_0(0) + \frac{i\beta_L\hbar\omega_0}{Z}\cdot\frac{1}{\hbar\omega_1'}\int_0^{\pi/2} d\theta e^{-ih_R(\pi/2-\theta)} \times \sum_k k d_{0k}(\theta)V^k e^{ih_R(\pi/2-\theta)} + \cdots, \quad [25]$$

where $\sigma_0(0) \cong (1 + \beta_L\hbar\omega_0 I_z + \cdots)/Z$ is the high temperature form of [2], Z is the partition sum, and $h_R = H_R/\hbar\omega_1'$, with $\omega_1' = \gamma_p H_1'$. The second term in [25] represents the sought-for modification of the initial condition [2] due to spin dephasing during the 90° pulse.

The Zeeman polarization along the x-axis of the laboratory frame is

$$M_x(t) = \gamma_p\hbar\,\mathrm{Tr}\{\rho(t)I_x\}, \quad [26]$$

or, in terms of the interaction picture density matrix $\sigma_I(t)$,

$$M_x(t) = \gamma_p\hbar\,\mathrm{Tr}\{\sigma_I(t)I_z\}\cos\omega_0 t + \gamma_p\hbar\,\mathrm{Tr}\{\sigma_I(t)e^{(i/\hbar)H_0 t}I_y e^{-(i/\hbar)H_0 t}\}\sin\omega_0 t. \quad [27]$$

The calculation of the traces in [27] is performed in the basis defined by [20] and is carried to the second order in dipolar interaction. To make the lengthy calculations a bit easier, we omitted a few terms of the order $(\omega_D/\omega_1')^2$ which contribute only to the Fourier peak centered at ω_1, whose dominant contributions are due to terms in [27] which are proportional to (ω_D/ω_1'). Furthermore, the presence of the rotational Hamiltonian H_R in the second term of [25] indicates that matrix elements of the type $\langle\nu_1 M|e^{(i/\hbar)H_R t}|\nu_2 M\rangle$ must be calculated. Even though H_R is strictly diagonal in the basis defined by [20] only in the limit $\omega_D/\Delta \to 0$, we will nevertheless replace such matrix elements by $e^{(i/\hbar)\langle\nu_1 M|H_R|\nu_2 M\rangle t}\delta_{\nu_1\nu_2}$. This simplifies the calculation and does not affect the results significantly.

Before presenting detailed results of the above calculation, let us examine the role of various terms in the equation of motion for $\sigma(t)$. Upon examination of [12] we attempt to

anticipate the time dependence of $M_x(t)$. The formal solution of [12] is $\sigma(t) = e^{(i/\hbar)(H_0+V)t}\sigma(0)e^{-(i/\hbar)(H_0+V)t}$. If we ignore the dipolar interaction term V and, moreover, retain just the first term in [25], then only the first term of [27] contributes. Thus, $M_x(t) = \gamma_p\hbar\mathrm{Tr}\{\sigma_0(0)I_z\}\cos\omega_0 t \equiv M_0\cos\omega_0 t$, representing the magnetization rotating in the x–y plane. When also the V-term is included in [12], while we continue to use the first term only of [25], it is more convenient to use the perturbation expansion [23] for calculation of traces in [27]. Since the states defined by [20] are eigenstates of I_z and, because the V^k terms contained in V as defined by [15] obey $[I_z, V^k] = kV^k$ it follows that V generates additional time-dependent terms which modulate $M_x(t)$. These terms oscillate with frequencies determined by the transitions among the eigenstates [20] induced by the various V^k terms. However, in the 90° tilted frame $d_{0\pm1} = 0$ as seen from [16b] and, consequently, up to the second order in V only the frequency $2\omega_1$ (shifted by the tunneling splitting Δ and H_D^{00} part of the dipolar interaction) will occur in $M_x(t)$. Again, only the first term of [27] gives nonzero contributions. Finally when, in addition, the second term of [25] (which includes the $V^{\pm1}$ terms as well) is used, the magnetization $M_x(t)$ acquires also modulations at frequency ω_1, generated by the second term of [27] and shifted similarly as $2\omega_1$ modulations. This is confirmed by the detailed and lengthy calculation which yields, for $2\omega_1' \gg \Delta$, the result

$$
\begin{aligned}
M_x(t) = M_0\cos\omega_0 t &- \sum_{\lambda=\pm} 4A_\lambda\left\{\frac{\omega_D^2[1-\cos(2\omega_1+\delta_\lambda)t]}{(2\omega_1+\delta_\lambda)^2}\right.\\
&\left.+\frac{\omega_D^2[1-\cos(2\omega_1-\delta_\lambda)t]}{(2\omega_1-\delta_\lambda)^2}\right\}\cos\omega_0 t\\
&+\sum_{\lambda=\pm}\left(\frac{\pi^2}{2}-2\right)A_\lambda\frac{c_\lambda^2\Delta}{\omega_1'}\\
&\times\left\{\frac{\omega_D^2[1-\cos(2\omega_1+\delta_\lambda)t]}{\omega_1'(2\omega_1+\delta_\lambda)}\right.\\
&\left.-\frac{\omega_D^2[1-\cos(2\omega_1-\delta_\lambda)t]}{\omega_1'(2\omega_1-\delta_\lambda)}\right\}\cos\omega_0 t\\
&-\sum_{\lambda=\pm}\pi A_\lambda\left\{\frac{\omega_D^2\sin(2\omega_1+\delta_\lambda)t}{\omega_1'(2\omega_1+\delta_\lambda)}\right.\\
&\left.+\frac{\omega_D^2\sin(2\omega_1-\delta_\lambda)t}{\omega_1'(2\omega_1-\delta_\lambda)}\right\}\cos\omega_0 t\\
&-\sum_{\lambda=\pm}\frac{9}{32}B_\lambda\left(\frac{\omega_D}{\omega_1'}\right)^2\{\cos(\omega_1+\delta_\lambda)t\\
&-\cos(\omega_1-\delta_\lambda)t\}\sin\omega_0 t-\sum_{\lambda=\pm}\left(\frac{\alpha_\lambda^2-1}{\alpha_\lambda}\right)A_\lambda B_\lambda\\
&\times\left\{\frac{\omega_D^2[\cos(\omega_1+\delta_\lambda)t-\cos\omega_1 t]}{\omega_1'(2\omega_1+\delta_\lambda)}\right.\\
&\left.-\frac{\omega_D^2[\cos(\omega_1-\delta_\lambda)t-\cos\omega_1 t]}{\omega_1'(2\omega_1-\delta_\lambda)}\right\}\sin\omega_0 t\\
&-\sum_{\lambda=\pm}\left(\frac{\alpha_{-\lambda}\alpha_\lambda-1}{\alpha_\lambda}\right)A_{-\lambda}B_\lambda\\
&\times\left\{\frac{\omega_D^2[\cos(\omega_1+\delta_\lambda)t-\cos(\omega_1-2\lambda b^{1/2})t]}{\omega_1'(2\omega_1+\delta_\lambda-2\lambda b^{1/2})}\right.\\
&\left.-\frac{\omega_D^2[\cos(\omega_1-\delta_\lambda)t-\cos(\omega_1+2\lambda b^{1/2})t]}{\omega_1'(2\omega_1-\delta_\lambda+2\lambda b^{1/2})}\right\}\\
&\times\sin\omega_0 t. \qquad [28]
\end{aligned}
$$

The symbols used above are defined in [21]. We have introduced also

$$\delta_\lambda = \tfrac{1}{2}\Delta + 3a + \lambda b^{1/2},\ \lambda = \pm, \qquad [29a]$$

$$A_\lambda = \tfrac{9}{256}M_0c_\lambda^2[-\alpha_\lambda(1-3\cos^2\beta)+3\sin^2\beta]^2, \qquad [29b]$$

$$B_\lambda = \tfrac{1}{6}M_0\alpha_\lambda c_\lambda^2[2\alpha_\lambda(1-3\cos^2\beta)+3\sin^2\beta. \qquad [29c]$$

To represent these results graphically, it is best to define the Fourier transform of $M_x(t)$ as

$$m_x(\omega, \cos\beta) = \frac{1}{\sqrt{2\pi}}\int_{-\infty}^{\infty} dt M_x(t)e^{i\omega t}. \qquad [30]$$

The expression for a polycrystalline sample is

$$\langle m_x(\omega)\rangle = \tfrac{1}{2}\int_{-1}^{1} d\cos\beta\, m_x(\omega, \cos\beta). \qquad [31]$$

Using [28], [29], and [30], $\langle m_x(\Omega)\rangle$, where $\Omega \equiv \omega - \omega_0$, is calculated. By broadening the spectra with a Gaussian broadening function according to

$$\langle m_x(\Omega;\sigma)\rangle = \frac{1}{\sqrt{2\pi\sigma^2}}\int_{-\infty}^{\infty} du\langle m_x(u)\rangle e^{-(\Omega-u)^2/2\sigma^2}, \qquad [32]$$

Figures 1a and 1b are obtained. To make these spectra easily comparable with the experimental ones, the figures are plotted as functions of the off-field parameter $h \equiv \Omega/\gamma_p$, instead of frequency.

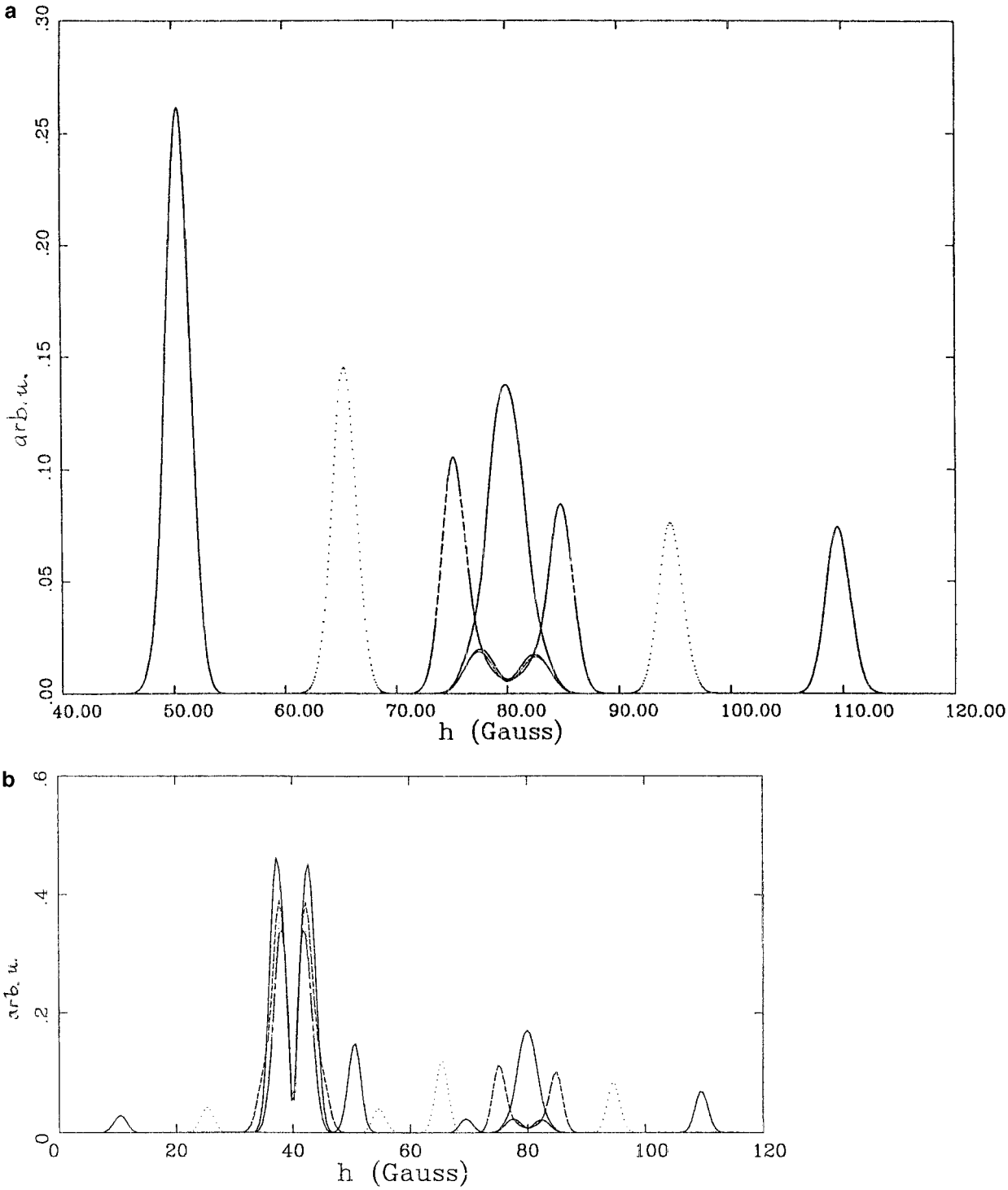

FIG. 1. (a) The absolute value of the real part of the Fourier transform of Expression [28]. In these graphs $H_1 \equiv \omega_1/\gamma_p = 40$ G, the strength of the 90° pulse is $H_1' \equiv \omega_1'/\gamma_p = 50$ G, and $\omega_D/\gamma_p = 5$ G. The tunneling parameter Δ/γ_p was chosen to be 0, 5, 15 (dotted lines), and 30 G. The curves are plotted as functions of Ω/γ_p. The intensity is given in arbitrary units. The broadening parameter $\sigma = 1$ G. Only the $\Delta M = 2$ peak and its satellites at ± 5, 15, and 30 G are shown since the $\Delta M = 1$ peak is zero for the real component. (b) The absolute value of the imaginary component of the Fourier transform of [28]. The tunneling parameter Δ/γ_p is 0, 5, 15, and 30 G, respectively. The remaining parameters are the same as in (a). It should be noted that even in the most careful spin-locking experiment a small missalignment of M_0 along H_1 cannot be avoided. As a result, experimentally, a small part of M_0 is precessing around H_1. This precession at ω_1 contributes a strong, experimentally observed peak at H_1 whose intensity dependence is shown in Fig. 2.

DISCUSSION OF THE RESULTS AND COMPARISON WITH EXPERIMENTS

It is well known (*7*) that the Fourier transform of Zeeman polarization in the rotating frame at exact resonance shows a nonvanishing intensity only in the vicinity of $2H_1$, where H_1 is the magnitude of the spin-locking field pulse (we are interested only in the Fourier components which are peaked at H_1 and $2H_1$. We neglect the Fourier component at $\Omega = 0$, which is always present, but is also always distorted because of experimental limitations). However, when the evolution of the Zeeman-rotational system during the 90° pulse is also accounted for, the Fourier transform acquires a nonzero intensity at H_1 as well. The intensity is proportional to $\beta_Z|H_Z|(\hbar\omega_D/\hbar\omega_1')$. This structure disappears in the limit $H_1' \to \infty$. In practice it is barely observable when H_1' is ≈60 G.

In Fig. 1a we show the absolute value of the real part of the Fourier transform of the Zeeman polarization in the rotating frame at exact resonance for various values of the tunneling parameter Δ. These results are in agreement with the results discussed previously (*7*). The structure of the peak centered at $2H_1$ was studied also for values of Δ which are small compared to ω_D, a case not treated in (*7*). We found that the effect of tunneling splitting is already noticeable when Δ is much smaller than ω_D. Furthermore, the real part of the Fourier transform does not depend much on the magnitude of the preparation pulse, at least for the Δ considered. For example, the spectra in Fig. 1 did not change when a fictitiously high $H_1' = 1$ K G was used in the calculation.

The imaginary component shown in Fig. 1b, has, unlike the real component, a nonvanishing intensity both at H_1 and at $2H_1$. However, the intensity of the H_1 peak is proportional to $1/H_1'$ and thus goes to zero in the limit of a strong 90° pulse. The structure and the relative intensity of the peak centered at $2H_1$ (where $H_1' = 50$ G and $H_1 = 40$ G) is roughly the same as the structure and relative intensity of the real component, but is weaker than the intensity of the peak centered at H_1 by a factor of ≈3. The tunneling side bands are seen adjacent to both peaks.

As was already pointed out, the real component of the Fourier transform $\langle m_x(\Omega;\ \sigma)\rangle$ at exact resonance shows a nonvanishing intensity only in the neighborhood of $2H_1$. Specifically, at $\Delta = 0$ there is a single peak centered at $2H_1$ with a width of 3.8 G at half intensity. As the tunneling splitting $\hbar\Delta$ increases, a double peak structure appears at relatively small values of Δ. The peak-to-peak separation of the resulting tunneling satellites is, over the whole range of Δ, given by Δh(peak to peak) $\cong (2\Delta + \omega_D/5)/\gamma_p$ for $\Delta \le \omega_D$ and Δh(peak to peak) $\cong (2\Delta - \omega_D/5)/\gamma_p$ for $\Delta > \omega_D$. At Δ/γ_p roughly equal to 6 G a dipolar double peak of fairly low intensity emerges from underneath the receding tunneling sidebands. The peak to peak distance of this dipolar line is ≅5 G. It is also observed that the intensity of the tunneling satellites on the low field side is higher than the corresponding intensity on the high field side, in agreement with the general results presented in the previous section.

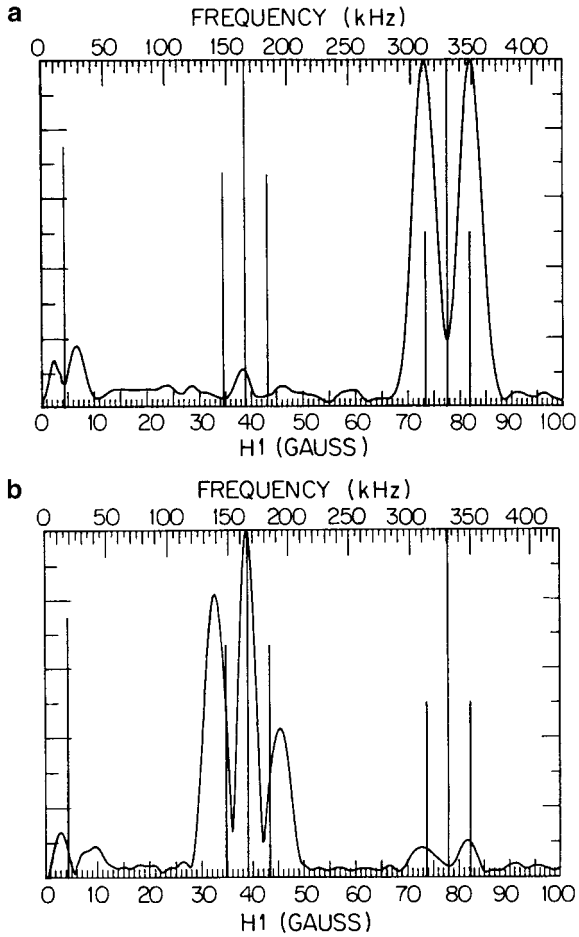

FIG. 2. The experimental CH_3CD_2I proton magnetization evolution on resonance. The real (absorption) component of its Fourier transform, a, and the imaginary (dispersion) component, b, detected in two separate channels are shown. Note the strong $\Delta M = 1$ peak at $H_1 = 39$ G with which the H_1 is determined. The tunneling parameter Δ/γ_p is 4.2 ± 0.2 G. Note also that the satellites of the $\Delta M = 1$ peak are split more due to the dipolar contribution, which is in this case significant in comparison with the small Δ. As Δ increases, the dipolar shifts of the $\Delta M = 1$ satellites become relatively smaller. The $\Delta M = 2$ satellites are shifted by ±Δ.

Unlike the real component, the imaginary component of $\langle m_x(\Omega;\ \sigma)\rangle$ shows a nonzero intensity both at H_1 and at $2H_1$. The structure of the peak centered at $2H_1$ together with its tunneling satellites is almost identical to the structure of the real component. Also the peak-to-peak distance of the tunneling satellites obeys the same relationship as given above. Figure 1b shows that the imaginary component of $\langle m_x(\Omega;\ \sigma)\rangle$ is characterized by a relatively strong double peak with a sharp cusp centered at H_1. At $\Delta = 0$ its intensity is three times larger than the intensity of the peak at $2H_1$. The peak-to-peak distance at H_1 is roughly 5.1 G when $\Delta = 0$, and drops to 4 G when $\Delta \ge 6$ G. The tunneling satellites become visible at $\Delta \approx$ 5 G and their separation is Δh(peak to peak) $\cong (2\Delta - \omega_D/5)\gamma_p$,

for $5 \leq \Delta \leq 20$ G. The dipolar interaction shifts the tunneling satellites corresponding to $|\Delta M| = 1$ and 2 by the same amount.

If we compare the results shown in Fig. 1 with the experimental Fourier transform of the Zeeman polarization obtained for CH_3CD_2I at 40 K with $H_1 = 38.76$ G (Fig. 2), the agreement between the calculated spectra and the experiment is reasonable.

To conclude we would like to emphasize that the magnetization given by [27] is evaluated immediately after the end of the field pulse H_1. However, the recording of the FID signal is delayed by a time τ (≈ 10 μs) after the end of the field pulse. For this reason we should have taken into account also the evolution of the magnetization in the laboratory frame under the action of $-\hbar\omega_0 I_z + H_R + H_D^0$ (here only the secular part of the dipolar interaction as defined in the laboratory frame is to be considered). A calculation entirely analogous to the one described above shows that the real and imaginary components of the Fourier transform of $\langle I_x(t + \tau)\rangle$ become mixtures of the real and imaginary parts as defined on the basis of [27]; see also (*12*). The corresponding weight factors are rapidly oscillating functions of the time delay τ. When comparing the calculated spectra [28] with the experiment this fact should be kept in mind. Moreover the τ-evolution causes the appearance of a new "nonmagnetic" peak centered at the off-field value corresponding to the tunneling frequency $\omega_T \equiv \Delta$ the intensity of which is comparable to the intensity of the line centered at $2H_1$; see (*9*) and (*13*).

In summary, we have shown that the approach to semiequilibrium in the spin rotating frame depends, in general, also on the 90° RF pulse amplitude. In particular, the Fourier transform of Zeeman polarization in the rotating frame at exact resonance shows a nonvanishing intensity not only at $2H_1$, where H_1 is the magnitude of the spin-locking field pulse, but at H_1 as well.

ACKNOWLEDGMENT

Support from Natural Sciences and Engineering Research Council (Ottawa) is gratefully appreciated.

REFERENCES

1. W. Press, "Single Particle Rotations in Molecular Crystals, Springer Tracts in Modern Physics," Springer-Verlag, Berlin, (1981).
2. J. A. Ripmeester, S. K. Garg, and D. W. Davidson, *J. Chem. Phys.* **67,** 2275 (1977).
3. R. S. Hallsworth, D. W. Nicoll, J. Peternelj, and M. M. Pintar, *Phys. Rev. Lett.* **39,** 1493 (1977).
4. C. Choi and M. M. Pintar, *Phys. Rev. B* **56,** 5954 (1997).
5. C. P. Slichter, "Principles of Magnetic Resonance—Third Enlarged and Updated Edition," Springer-Verlag, Berlin (1990).
6. S. Clough, A. J. Horsewill, P. J. McDonald, and F. O. Zelaya, *Phys. Rev. Lett.* **55,** 1794 (1985).
7. D. W. Nicoll and M. M. Pintar, *Phys. Rev. B* **23,** 1064 (1981).
8. J. Peternelj, A. Damyanovich, and M. M. Pintar, *Phys. Rev. Lett.* **82,** 2587 (1999).
9. P. S. Hubbard, *Rev. Mod. Phys.* **33,** 249 (1961).
10. R. E. Andrew and R. Bersohn, *J. Chem. Phys.* **18,** 159 (1950).
11. F. Apaydin and S. Clough, *J. Phys. C* **1,** 932 (1968).
12. J. Peternelj, A. Damyanovich, and M. M. Pintar, *Phys. Rev. B* **49,** 3322 (1994).
13. M. J. Barlow, S. Clough, P. A. Debenham, and A. J. Horsewill, *J. Phys. C* **4,** 4165 (1992).